Stability of Phosphonic Acid Self-Assembled Monolayers on Amorphous and Single-Crystalline Aluminum Oxide Surfaces in Aqueous Solution

3 AUTHORS:

Peter Thissen
Karlsruhe Institute of Technology
33 PUBLICATIONS **489** CITATIONS
SEE PROFILE

Markus Valtiner
Max Planck Institute for Iron Research GmbH
54 PUBLICATIONS **510** CITATIONS
SEE PROFILE

G. Grundmeier
Universität Paderborn
117 PUBLICATIONS **1,806** CITATIONS
SEE PROFILE

Langmuir
Article
pubs.acs.org/Langmuir

Stability of Phosphonic Acid Self-Assembled Monolayers on Amorphous and Single-Crystalline Aluminum Oxide Surfaces in Aqueous Solution

Peter Thissen,[†,‡] Markus Valtiner,*[,†,‡] and Guido Grundmeier[†,‡]

[†]*Christian Doppler Laboratory for Polymer/Metal Interfaces at the Max-Planck-Institut für Eisenforschung GmbH, Max-Planck-Str. 1, D-40237 Düsseldorf, Germany and* [‡]*Department of Technical and Macromolecular Chemistry, University of Paderborn, Warburger Str. 100, D-33098 Paderborn, Germany*

Received March 17, 2009. Revised Manuscript Received September 7, 2009

The formation of octadecylphosphonic acid (ODPA) self-assembled monolayers (SAMs) and their stability in water has been studied on four distinctly different aluminum oxide surfaces. The aim was to improve the understanding of the state of binding between the phosphonic acid to the oxide surface and how this interaction depends on the structure and termination of the oxide surface. Single crystalline $Al_2O_3(0001)$ and $Al_2O_3(1\bar{1}02)$ surfaces were compared to amorphous oxide passive films on aluminum and physical vapor deposited (PVD) amorphous aluminum oxide films on gold. The monolayers were adsorbed from ethanol solution, characterized by means of high-resolution in situ atomic force microscopy (AFM), contact angle measurements, polarization modulated infrared reflection absorption spectroscopy (PM-IRRAS), and diffuse reflectance infrared Fourier transform spectroscopy (DRIFTS), and proved to be self-assembled. On $Al_2O_3(1\bar{1}02)$ surfaces and amorphous Al_2O_3 surfaces, the ODPA self-assembled monolayers showed high stability in aqueous environments. However, the adsorbed ODPA monolayers were substituted by the adsorption of interfacial water on the $Al_2O_3(0001)$ surface via the intermediate formation of micelles. The different stability of the monolayers in aqueous environments is explained by the variation of interfacial binding states ranging from ionic interactions between phosphonate groups and the positively charged hydrolytated oxide surface to directed coordination bonds between the phosphonate group and Al ions.

Introduction

Molecular adhesion forces at interfaces between organic coatings or adhesives and engineering metals are governed by physisorption or chemisorption of macromolecules or adhesion promoting additives on these passive film surfaces. In this context, an understanding of the surface chemistry as well as molecular binding mechanisms on a fundamental level is important for adhesion promotion on oxide covered metal substrates.[1,2] As almost all engineering metals are covered by a native oxide film, especially the combined understanding of the structure of these oxide films as well as their corresponding interface chemistry in the presence of macromolecules is of crucial importance for the design of polymer/metal composites.[3−5] Aluminum alloys, which are covered by a passive oxide film, are used in wide range of applications ranging from the aviation industry to the automotive and construction industries. Adhesive joining of such alloys and the application of organic coatings for corrosion protection are of high technological importance.[4,6−8]

The adsorption of phosphonic acid self-assembled monolayers (SAMs) on aluminum oxide surfaces is of substantial interest, because α-ω-bifunctional phosphonate monolayers have been shown to act as adhesion promoting molecules.[3] The bifunctionality enables the binding of the phosphonic acid or its anion to the oxide surface while the second group (e.g., amine or epoxy) leads to a chemical binding reaction with the organic phase of the adhesive or coating. It could be shown that organophosphonic acids form very stable monolayer on aluminum alloys covered with an amorphous thin oxide film.[6,9−13] Several recent studies focused on engineering aspects of the related interfacial chemistry.[14−16] It could be shown that the adsorption rate of octadecylphosphonic acid (ODPA) is strongly dependent on the OH density of the surface which can be influenced by plasma modification.[16] Maege et al. investigated the adhesion of different organophosphonates on aluminum alloys and assumed an acid−base interaction with a tridentate binding.[15] Wapner et al. used short a chain aminopropylphosphonic acid (APPA) as adhesion promoting molecule on aluminum alloy surfaces and showed that they can be also used as additives in adhesives.[14] In comparison with carboxylic acid self-assembly films, the increased binding

*To whom correspondence should be addressed. Telephone: +49/211/6792-447. E-mail: valtiner@mpie.de.

(1) Wilson, B.; Fink, N.; Grundmeier, G. *Electrochim. Acta* **2006**, *51*(15), 3066–3075.
(2) Fink, N.; Wilson, B.; Grundmeier, G. *Electrochim. Acta* **2006**, *51*(14), 2956–2963.
(3) Grundmeier, G.; Schmidt, W.; Stratmann, M. *Electrochim. Acta* **2000**, *45* (15−16), 2515–2533.
(4) Grundmeier, G.; Stratmann, M. *Annu. Rev. Mater. Res.* **2005**, *35*, 571–615.
(5) Grundmeier, G.; Stratmann, M. *Appl. Surf. Sci.* **1999**, *141*(1−2), 43–56.
(6) Foster, T. T.; Alexander, M. R.; Leggett, G. J.; McAlpine, E. *Langmuir* **2006**, *22*(22), 9254–9259.
(7) Liakos, I. L.; Newman, R. C.; McAlpine, E.; Alexander, M. R. *Surf. Interface Anal.* **2004**, *36*(4), 347–354.
(8) Lewington, T. A.; Alexander, M. R.; Thompson, G. E.; McAlpine, E. *Surf. Eng.* **2002**, *18*(3), 228–232.
(9) Luschtinetz, R.; Oliveira, A. F.; Frenzel, J.; Joswig, J. O.; Seifert, G.; Duarte, H. A. *Surf. Sci.* **2008**, *602*(7), 1347–1359.
(10) Raman, A.; Dubey, M.; Gouzman, I.; Gawalt, E. S. *Langmuir* **2006**, *22*(15), 6469–6472.
(11) Adolphi, B.; Jahne, E.; Busch, G.; Cai, X. D. *Anal. Bioanal. Chem.* **2004**, *379*(4), 646–652.
(12) Textor, M.; Ruiz, L.; Hofer, R.; Rossi, A.; Feldman, K.; Hahner, G.; Spencer, N. D. *Langmuir* **2000**, *16*(7), 3257–3271.
(13) Woodward, J. T.; Ulman, A.; Schwartz, D. K. *Langmuir* **1996**, *12*(15), 3626–3629.
(14) Wapner, K.; Stratmann, M.; Grundmeier, G. *Int. J. Adhes. Adhes.* **2008**, *28* (1−2), 59–70.
(15) Maege, I.; Jaehne, E.; Henke, A.; Adler, H. J. P.; Bram, C.; Jung, C.; Stratmann, M. *Prog. Org. Coat.* **1998**, *34*(1−4), 1–12.
(16) Giza, M.; Thissen, P.; Grundmeier, G. *Langmuir* **2008**, *24*(16), 8688–8694.

stability of phosphonic acids with oxide surfaces[11] triggers an increasing interest in phosphonic acid SAMs for applications in many other fields such as microelectronics and biosensors[17] to name but a few. In recent literature, the main issue was to understand and prove the SAM formation of phosphonic acids on alumina surfaces.[9,18,19] Solution chemistry was shown to have a strong impact on the quality of the formed SAMs. In water based solutions, phosphonic acids tend to form molecular bilayers.[20,21]

Despite the considerable interest in phosphonic acid self-assembly on alumina[18] and extensive studies of the self-assembly process,[13] only little is know about the nature of the chemical binding of phosphonic acids to aluminum oxide surfaces[22] and their long-term stability against desorption in competition with water. This is, however, one of the most important issues toward an improvement of adhesive technology based on phosphonate adhesion promoters.[4] It is essential to understand the binding mechanisms on different oxide surfaces as well as the kinetics of individual processes taking place during the self-assembly as well as during aging and de-adhesion of phosphonic acid interfacial layers. In this context, the stability of the formed monolayer in the presence of high water activities is of high practical interest for improving wet-adhesion and corrosion resistance. Water adsorption as such has been studied quite intensively on different single crystal aluminum oxide surfaces by theoretical[23−25] as well as experimental methods.[26,27]

The focus of the presented study was to improve the knowledge of the binding of organophosphonic acid molecules on aluminum oxide surfaces by studying a selected series of aluminum oxide surfaces with distinctly different morphologies and atomistic structures. The combined study of two different amorphous surface oxide films on aluminum and gold as well as two different single-crystalline aluminum oxide surfaces with respect to the adsorption and desorption of ODPA-SAMs allowed a differential understanding of the interfacial binding and desorption mechanisms in aqueous environments.

Experimental Section

Sample Preparation. Four different types of aluminum oxide surfaces were used and coated with a monolayer of ODPA molecules. All chemical reagents were of analysis grade and were used without any further purification. The different sample types were prepared as follows:

Type 1. Pure aluminum samples (Al 99.99%) were prepared by melting and casting the metal under argon atmosphere. Afterward, the samples were cut into pieces of $10 \times 10 \times 3\ mm^3$, and the surface was polished with diamond paste of a corn radius of 1 μm and ultrasonically cleaned in absolute ethanol (> 99.9%, Merck, Germany) for 10 min. After rinsing with ethanol, the samples were dried in a stream of nitrogen. The rms roughness of these samples was below 3 nm/μm^2. The native grown oxide on these samples is typically a pseudo-bohemite phase.[28]

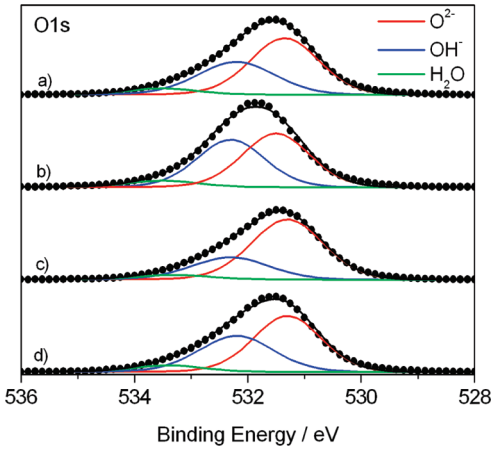

Figure 1. All spectra were referenced to the aliphatic C1s peak at 285 eV binding energy. O1s core level spectra of a (a) native oxide covered aluminum surface, (b) physical vapor deposited oxide covered aluminum surface, (c) single-crystalline $Al_2O_3(1\bar{1}20)$ surface, and (d) single-crystalline $Al_2O_3(0001)$ surface are shown.

Type 2. Pure aluminum oxide layers were deposited onto Au-coated (100 nm, with an adhesion promotion layer of 2 nm Cr) silicon wafer substrates by means of physical vapor deposition of Al_2O_3 (Univex 450, Leybold AG). During evaporation, the layer thickness was monitored by using a quartz crystal microbalance (QCM; Inficon XTC). Prior to film deposition, the samples were thoroughly cleaned in a mixture of hydrogen peroxide (30%, Merck, Germany) and ammonia (25%, Merck, Germany) (1:1) for 60 min at 80 °C and afterward rinsed with deionized (DI) water and dried in a stream of nitrogen. To ensure a completely oxidized aluminum layer, the samples were further treated with an oxygen plasma after the deposition. The surface morphology of these samples was smooth with a rms roughness below 1 nm/μm^2.

Type 3 and 4. Sapphire wafers with the surface orientation (0001) and $(1\bar{1}02)$ were purchased from Mateck (Mateck GmbH, Germany). Before annealing, the crystals were immersed into 85% phosphoric acid for 1 min, rinsed with deionized water, and dried in a stream of nitrogen. The sapphire crystals were than annealed in ambient air at 1400 °C for 24 h. For the polar (0001) surfaces, these annealing conditions were shown to give hydroxide-stabilized $Al_2O_3(000\bar{1})$-Al surfaces.[23,29] The resulting surface structure of the $Al_2O_3(1\bar{1}20)$ oriented crystals was investigated by Trainor et al.[30] by means of crystal truncation rod studies. For both types, these annealing conditions led to surface morphologies with atomically flat terraces, whereas the step density is considerably higher on the nonpolar $(1\bar{1}20)$ surface (see Figures 4 and 5, respectively). Low energy electron diffraction (LEED) confirmed the atomic scale ordered structure on these surfaces (see Figure 8).

X-ray photoelectron spectroscopy (XPS) spectra in Figure 1 show a comparison of the O1s core-level spectra at 45° take-off angle of the photoelectrons for as-prepared surfaces. The curves could be fitted with three species of oxygen: in the form of adsorbed water (533.3 eV), hydroxide (532.3 eV), and oxidic oxygen (531.3 eV). In Table 1, chemical composition and deconvoluted data of the C1s and O1s spectra are shown for the different sample types at low and standard take-off angles.

(17) Wink, T.; van Zuilen, S. J.; Bult, A.; van Bennekom, W. P. *Analyst* **1997**, *122*(4), R43–R50.
(18) Hoque, E.; DeRose, J. A.; Hoffmann, P.; Mathieu, H. J.; Bhushan, B.; Cichomski, M. *J. Chem. Phys.* **2006**, *124*(17), 174710.
(19) Forget, L.; Wilwers, F.; Delhalle, J.; Mekhalif, Z. *Appl. Surf. Sci.* **2003**, *205* (1−4), 44–55.
(20) Hauffman, T.; Blajiev, O.; Snauwaert, J.; van Haesendonck, C.; Hubin, A.; Terryn, H. *Langmuir* **2008**, *24*(23), 13450–13456.
(21) Hauffman, T.; Jorcin, J. B.; Ingelgem, Y. V.; Breugelmans, T.; Tourwe, E.; Hubin, A.; Vereecken, J. *Mater. Tech.* **2007**, 411–415.
(22) Pertays, K. M.; Thompson, G. E.; Alexander, M. R. *Surf. Interface Anal.* **2004**, *36*(10), 1361–1366.
(23) Wang, X. G.; Chaka, A.; Scheffler, M. *Phys. Rev. Lett.* **2000**, *84*(16), 3650–3653.
(24) Hass, K. C.; Schneider, W. F.; Curioni, A.; Andreoni, W. *J. Phys. Chem. B* **2000**, *104*(23), 5527–5540.
(25) Ranea, V. A.; Schneider, W. F.; Carmichael, I. *Surf. Sci.* **2008**, *602*(1), 268–275.
(26) Elam, J. W.; Nelson, C. E.; Tolbert, M. A.; George, S. M. *Surf. Sci.* **2000**, *450*(1−2), 64–77.
(27) Nelson, C. E.; Elam, J. W.; Cameron, M. A.; Tolbert, M. A.; George, S. M. *Surf. Sci.* **1998**, *416*(3), 341–353.
(28) Alexander, M. R.; Thompson, G. E.; Beamson, G. *Surf. Interface Anal.* **2000**, *29*(7), 468–477.
(29) Barth, C.; Reichling, M. *Nature* **2001**, *414*(6859), 54–57.
(30) Trainor, T. P.; Eng, P. J.; Brown, G. E.; Robinson, I. K.; De Santis, M. *Surf. Sci.* **2002**, *496*(3), 238–250.

Table 1. Sample Composition and Deconvolution of Detailed XPS Spectra of C1s and O1s Peaks at Different Take-Off Angles

			O1s (%)				C1s (%)			
type of oxide	take-off-angle (°)	Al2p (%)	total	O^{2-}	OH	H_2O	total	C—C	C—O	C=O
type I oxide covered Al	10	16.8	48.3	12.1	28.5	7.7	34.9	28.9	4.4	1.6
	45	29.5	61.2	30.7	26.9	3.6	9.3	7.6	1.2	0.5
type II amorphous Al_2O_3	10	17.1	51.1	15.9	27.4	7.8	31.8	25.4	4.4	2.0
	45	30.7	61.1	34.8	22.5	3.8	8.2	6.7	1.1	0.3
type III $Al_2O_3(0001)$	10	22.3	55.0	16.9	29.7	8.4	22.7	17.9	3.5	1.3
	45	34.3	58.2	32.0	22.5	3.7	7.5	6.2	0.9	0.4
type IV $Al_2O_3(1\bar{1}20)$	10	23.3	55.0	20.1	26.4	8.5	21.6	19.0	1.8	0.8
	45	32.3	62.2	42.6	16.7	2.9	5.5	4.8	0.5	0.2

The hydroxide content increases with the lower take-off angle of 10°, indicating the presence of the hydroxide on the surface. The atmospheric carbon contamination consisted mainly of aliphatic carbon, and thus, the oxygen containing contaminations were neglected for analyzing the hydroxide fractions.[31] The O/OH fraction of the type 4 $Al_2O_3(1\bar{1}20)$ surface is 2.5, which is significantly higher compared to the other three sample types, which have a comparable O/OH ratio between 1.2 and 1.5. This is consistent with the expected structure of the surfaces. On the one hand, type 1 and 2 surfaces consist of a pseudo-bohemite phase[28] and the polar $Al_2O_3(0001)$-Al surface is necessarily stabilized by the presence of hydroxides.[23] The reconstructed $Al_2O_3(1\bar{1}20)$ surface on the other hand features a stochiometric surface composition with less protonated surface oxygens.[30] In general, the presence of hydroxides at the surface is known to increase the adsorption kinetics of phosphonic acids, but the stability of the binding is not strongly affected by surface hydroxides as discussed by Giza et al.[16]

ODPA monolayers on the four types of aluminum oxide surfaces were prepared by solution self-assembly under ambient conditions. Substrates were ultrasonically cleaned in absolute ethanol (>99.9%, Merck, Germany) for 10 min before immersing into a 1 mM ethanolic solution of ODPA for 24 h (see Whitesides et al.[32] for general information). Afterward, the samples were thoroughly rinsed with ethanol and dried in a stream of nitrogen.

Static Contact Angle Measurements. The static contact angle of water was measured by means of the sessile-drop method using an OCA 20 goniometer (Dataphysics, Germany).

Atomic Force Microscopy (AFM). AFM topography experiments were performed with a JPK NanoWizards atomic force microscope (JPK Instruments AG, Berlin, Germany) using a custom-made liquid cell. The system is equipped with a homemade antinoise and antivibration box. The *z*-piezo of the AFM instrument was calibrated with a 1-D array of rectangular SiO_2 steps with a height of 18.6 nm (TGZ01 from m-Masch). The *xy*-piezos were internally calibrated with integrated capacitive position sensors. The in situ images were recorded in constant force and constant amplitude mode using silicon sensors (CONTR obtained from NanoWorld, typical tip radius less than 10 nm, $k = 0.1-0.3$ N/m). In constant force mode, the force set point was allowed to be at maximum 2 nN in order to minimize any scanning induced effects. In constant amplitude mode, the amplitude was damped to 90% with respect to the free amplitude.

Polarization Modulation Infrared Reflection Absorption Spectroscopy (PM-IRRAS). PM-IRRAS measurements were performed on a step scan interferometer (Bruker Vertex 70) at a resolution of 4 cm^{-1} and 80° relative to the substrate surface normal. For p-polarization of the IR light, an aluminum wire grid was used and modulated at 100 kHz with a ZnSe photoelastic modulator (PEM, Bruker PMA-50). Light reflected from the sample was focused with a ZnSe lens onto a cryogenic mercury cadmium telluride (MCT) detector. All presented spectra were recorded from 512 single scans. As reference, a respective clean alumina surface was used as background and subtracted from the sample data.

Diffuse Reflection Infrared Fourier Transform Spectroscopy (DRIFTS). DRIFT measurements were performed with the Harrick Praying Mantis measurement cell (continuously floated with nitrogen) in a Bruker V70 spectrometer with a deuterated triglycine sulfate (DTGS) detector. As reference, the respective clean alumina surface was used as background and subtracted from the sample data. The resolution of the presented data is 4 cm^{-1}, and 512 scans were integrated for each measurement.

Results

The fundamental approach was to combine analytical studies of the adsorption as well as desorption of ODPA in competition with water on a series of selected aluminum oxide surfaces, which differ in their atomic arrangements and electronic structure. This concept allowed a comparative understanding of the interfacial chemistry between the adsorbing phosphonic acid and the aluminum oxide especially with respect to the competition with water adsorption on the oxide surface.

Two different amorphous surfaces, which only differed in the supporting bulk substrate, were studied. One system consisted of a native oxide film with a thickness of 2−3 nm[33] as grown on aluminum under atmospheric conditions. For comparison, a 250 nm thick evaporated amorphous aluminum oxide film was deposited on a Au-coated silicon wafer surface. As single-crystalline substrates, two different single-crystalline sapphire surfaces with a distinctly different local geometry of the atomic arrangements were used. The polar $Al_2O_3(0001)$ surface and the nonpolar $Al_2O_3(1\bar{1}02)$ surface were used. Both surface orientations were intensively discussed in the literature with an emphasis on the $Al_2O_3(0001)$ orientation.[24−27,29,30] The behavior of adsorbed ODPA monolayers was analyzed on all these surfaces, allowing the comparative understanding of the adsorption and desorption chemistry in competition with water.

The formation of the ODPA-SAM was characterized by means of PM-IRRAS on the amorphous films on metal substrates and DRIFTS on the single-crystalline oxides. Desorption in aqueous solution was comparatively investigated by means of AFM, static contact angle measurements, as well as DRIFTS and PM-IRRAS measurements. In the following, the results on the different surfaces are presented and finally commonly discussed in terms of a comparative study.

(31) Wielant, J.; Hauffman, T.; Blajiev, O.; Hausbrand, R.; Terryn, H. *J. Phys. Chem. C* **2007**, *111*(35), 13177–13184.
(32) Love, J. C.; Estroff, L. A.; Kriebel, J. K.; Nuzzo, R. G.; Whitesides, G. M. *Chem. Rev.* **2005**, *105*, 1103–1169.
(33) Frerichs, A.; Voigts, F.; Maus-Friedrichs, W. *Appl. Surf. Sci.* **2006**, *253*(2), 950–958.

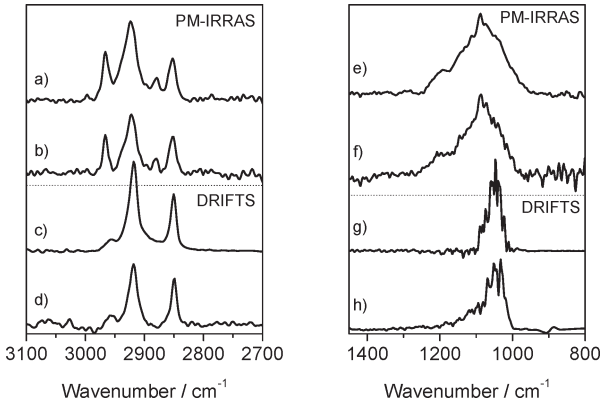

Figure 2. (a,e) PM-IRRAS data of an ODPA monolayer adsorbed on oxide covered aluminum in the corresponding wavelength regions; (b,f) PM-IRRAS spectrum of an ODPA monolayer adsorbed on PV deposited aluminum oxide; (c,g) DRIFTS data of ODPA adsorbed on an $Al_2O_3(0001)$ single crystal, corresponding wavelength regions; (d,h) DRIFTS of monolayer on $Al_2O_3(1\bar{1}02)$ single crystal surface.

Adsorption of ODPA Monolayers on Aluminum Oxide Surfaces. In general, mean orientation, packing density, and interfacial bond formation of the self-assembled monolayer can be analyzed by means of grazing incidence Fourier transform infrared (FTIR) spectroscopy. In the present case, PM-IRRAS is suitable only for the analysis of ODPA monolayers on aluminum oxide films on a metal substrate as long as the IR light can be reflected from an underlying metal substrate. Therefore, only samples of type 1 and 2 could be analyzed by PM-IRRAS. For ODPA monolayers on single-crystalline oxide surfaces, diffuse reflectance spectroscopy, which does not require a reflecting metal substrate,[34] was performed. This method allows for the analysis of the interfacial bond formation as well. In contrast to PM-IRRAS, this technique does not contain information about the orientation of the self-assembled molecules.[34] In the following section, the spectra of ODPA monolayers formed on the four types of substrates are discussed. Spectra of the adsorbed films were compared to spectra of the free phosphonic acids measured by means of attenuated total reflection (ATR). The respective FTIR spectra are presented in Figure 2. The peak assignments are listed in Table 2.

PM-IRRAS data of the ODPA monolayer on native grown, oxide covered aluminum (Figure 2a,e) and aluminum oxide on a gold substrate (Figure 2b,f) show that ODPA could be immobilized as an organophosphonate self-assembled monolayer on these oxide surfaces based on the peak ratio and peak positions.[34] In particular, the spectral region of the CH_2 and CH_3 stretching vibrations shows that the peak ratio $A(CH_3)/A(CH_2)$ is significantly increased in the adsorbed state in comparison to a bulk spectrum of ODPA.[14,15] According to Tilman et al.,[35,36] this is a clear indication that the ODPA is not only forming a monolayer but that a self-assembly process takes place leading to a mean upright orientation of the aliphatic chain of the ODPA. The mean inclination angle can be derived from the peak ratio, and it was calculated according to the following equation (taken from ref 36):

$$\frac{I_{CH_2}}{I_{CH_3}} = \frac{n2\cos(90^\circ - \alpha)^2}{3\cos(35^\circ - \alpha)^2} \quad (1)$$

Table 2. Assignment of FTIR Peaks As Observed in the Spectra in Figure 1[a]

vibration mode	PM-IRRAS of ML on oxide covered Al	PM-IRRAS of ML on oxide covered Al	DRIFT of ML on $Al_2O_3(0001)$	DRIFT of ML on $Al_2O_3(1\bar{1}02)$	ref
$n_{as}(CH_3)$	2965	2966	2957	2958	15, 16
$n_{as}(CH_2)$	2923	2922	2918	2918	15, 16
$n_s(CH_3)$	2880	2879			15, 16
$n_s(CH_2)$	2853	2853	2850	2849	15, 16
n(P═O)	1194	1207		1190	15, 16
n(P−O)	1129	1137		1121	15, 16
$n_{as}(PO_3^{2-})$	1089	1085	1087	1069	15, 16
$n_s(PO_3^{2-})$	1046	1039	1049	1031	15, 16

[a] All values are given in cm^{-1}.

For ODPA adsorbed on oxide covered aluminum (type I sample) and aluminum oxide (type II sample), the mean inclination angle was calculated to be 30° ± (0.9°) in both cases..

Moreover, the phosphonic acid functionality appears to be deprotonated. In Figure 2e/f, it can be seen that the peaks of the free acid group (P−OH), which would appear within the range from 900 to 980 cm^{-1}, are absent. For further discussion, the broad phosphonate band with a maximum at about 1089 cm^{-1} was considered in more detail. It can be observed that the stretching peaks of the P═O group and the PO_3 group are present in the spectra of all ODPA films adsorbed on amorphous alumina. In combination with the studied stability toward desorption in aqueous environment, which will be discussed in detail below, one specific type of binding toward the alumina surfaces is most plausible. We conclude that the binding on both of the amorphous alumina is mainly governed by bidentate condensation of the phosphonate onto the respective oxide surfaces, which is consistent with the disappearance of the P−OH vibrations and the detected P═O stretching vibrations. Moreover, the formation of a multilayer, as experimentally seen by SAM adsorption from aqueous solutions,[20] is not indicated by these results. A multilayer could be detected as free phosphonic acid functionalities in the IR spectrum as well.

The DRIFT spectra of ODPA adsorbed on $Al_2O_3(0001)$ and $Al_2O_3(1\bar{1}02)$ are presented in Figure 2c,g and Figure 2d,h, respectively. These spectra indicate the surface immobilization of the phosphonate. Due to the physical principle of this scattering method, the signal of the CH_2/CH_3 vibrations within the range from 2800 to 3000 cm^{-1} does not contain orientation dependent information. Nevertheless, in this case, the shift of the peak positions is a clear indicator for the immobilization of an ODPA self-assembled monolayer on both single crystal surfaces. According to ref 34, SAM formation leads to a shift for $\nu_{asym}(CH_2) \leq 2920$ cm^{-1} and $\nu_{sym}(CH_2) \leq 2850$ cm^{-1}, which is observed in the presented spectra, indicating successful SAM formation on the respective substrates.

The spectral region of the phosphonate groups provides detailed information on the formed interfacial bonds as measured by DRIFTS. For the $Al_2O_3(0001)$, surface the spectrum (Figure 2g) indicates interfacial bond formation based on ionic binding between the deprotonated phosphonic acid group and the Al ions in the oxide surfaces, based on the disappearance of the peaks assigned to P−OH as well as P═O stretching vibrations. Only PO_3^{2-} stretching vibrations could be detected, which is consistent with an ionic binding mechanism. In contrast the

(34) Lim, M. S.; Feng, K.; Chen, X. Q.; Wu, N. Q.; Raman, A.; Nightingale, J.; Gawalt, E. S.; Korakakis, D.; Hornak, L. A.; Timperman, A. T. *Langmuir* **2007**, *23* (5), 2444–2452.

(35) Bram, C.; Jung, C.; Stratmann, M. *Fresenius' J. Anal. Chem.* **1997**, *358* (1−2), 108–111.

(36) Tillman, N.; Ulman, A.; Schildkraut, J. S.; Penner, T. L. *J. Am. Chem. Soc.* **1988**, *110*(18), 6136–6144.

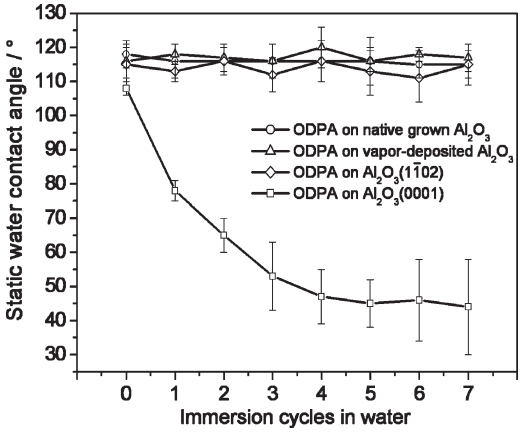

Figure 3. Static contact angle of water for ODPA adsorbed on native grown Al_2O_3 (○), vapor-deposited Al_2O_3 (△), single-crystalline $Al_2O_3(1\bar{1}02)$ (◇), and single-crystalline $Al_2O_3(0001)$ (□).

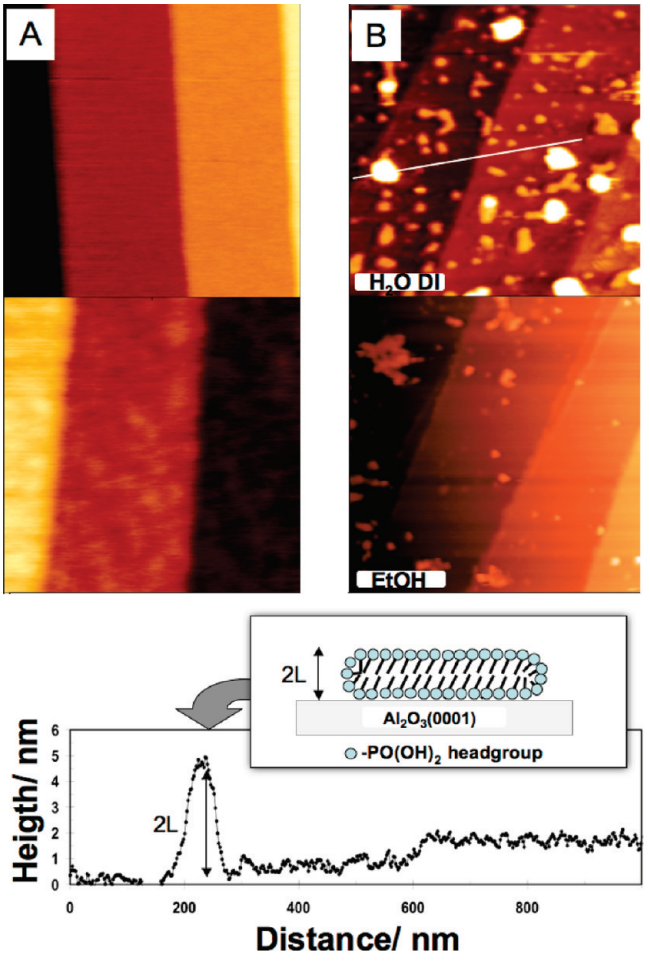

Figure 4. All images are 1 μm^2. (A) AFM topography of a single-crystalline $Al_2O_3(0001)$ surface (top) with and (bottom) without ODPA-SAM (both taken in EtOH). The step heights are typically about 1 nm. (B) (top) In situ AFM topography of ODPA-covered $Al_2O_3(0001)$ single crystal surface in water indicates formation of micellelike ODPA bilayer islands at the solid/liquid interface as indicated by the height histogram and within the model at the lower left corner. (bottom) Consequent in situ imaging in ethanol solution revealed that these micellelike islands can be dissolved.

spectra of the $Al_2O_3(1\bar{1}02)$ surface, Figure 2h still shows the presence of the asymmetric P−O vibration as well as weak P═O stretching vibrations, indicating a similar type of binding as

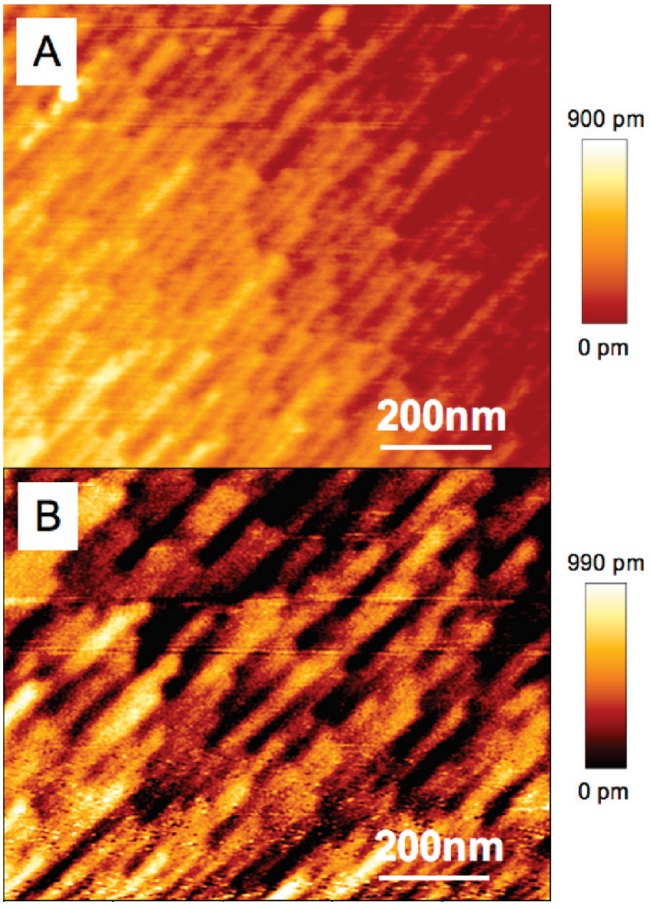

Figure 5. (A) AFM topography of a single-crystalline Al_2O_3-$(1\bar{1}02)$ surface with ODPA-SAM recorded in EtOH. (B) AFM topography of a single-crystalline $Al_2O_3(1\bar{1}02)$ surface with ODPA-SAM recorded after changing into aqueous medium. No significant structural differences or micelle formation could be detected.

concluded for both amorphous aluminum oxide films. Based on the presented FTIR data, interfacial binding appears to be based on a purely ionic mechanism only on the $Al_2O_3(0001)$ surface. On the other substrates, the binding mechanism of ODPA is most likely based on a bidentate condensation of ODPA onto the surfaces at suitable binding positions.

Stability of ODPA SAMs on Aluminum Oxide Surface in an Aqueous Environment. Molecular desorption of the self-assembled monolayers of ODPA was investigated by means of in situ AFM, water static contact angle measurements, and FTIR spectroscopy. In situ AFM was performed to image changes of the topography of the ODPA SAM on the respective Al oxide surface in an aqeuous solution. The contact angle measurements were done to provide information on the average surface energy which reflects the coverage and degree of orientation of the adsorbed ODPA monolayers. FTIR measurements led to information on the amount of adsorbed ODPA after immersion into aqueous solutions and the degree of orientation in the case of PM-IRRAS data.

Characterization and Stability by Static Water Contact Angle Measurements. Contact angle measurements were used to confirm the formation of self-assembly film on the various substrates. For three types of samples, the static contact angle after preparation of the SAM yielded high contact angles of 115−120°. Only the polar $Al_2O_3(0001)$ surface was leading to a slightly lower value of 108°. This is consistent with recent

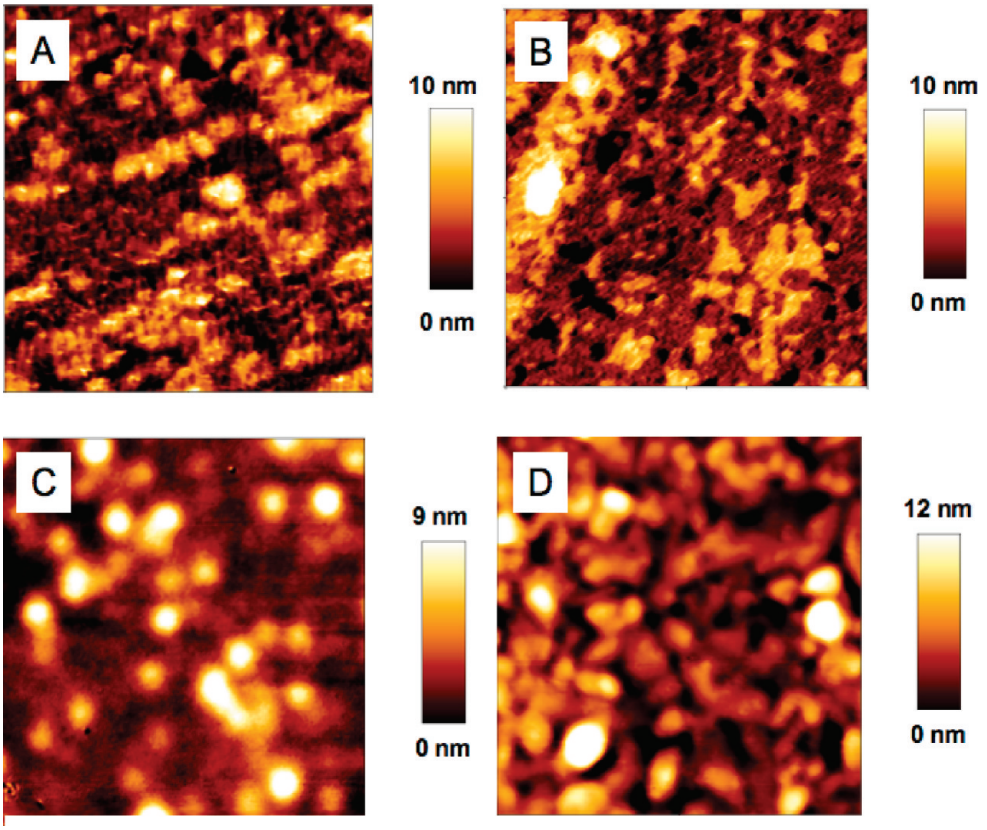

Figure 6. (A) AFM topography of an amorphous Al_2O_3 surface with ODPA-SAM. (B) AFM topography of an amorphous Al_2O_3 surface with ODPA-SAM recorded after changing into aqueous medium. No significant structural differences or micelle formation could be detected. (C) AFM topography of a native Al_2O_3 surface grown on bare aluminum covered with ODPA-SAM as recorded in EtOH. (D) AFM topography of the native grown Al_2O_3 after immersing into water. The surface topography changed significantly, leading to a roughening of the surface morphology. However, no micelles could be detected in situ. In comparison with the IR and contact angle data, this may indicate a possible corrosive attack at the Al/Al_2O_3 interface.

observation of Brukman et al.[37] who used similar preparation conditions of the crystal. Another study with differently pretreated crystals (shorter annealing time) gave lower values between 55 and 85°, which were assumed to result from different phases which coexist on the crystals.[38] In the present case, the slightly lower value compared to those of the other substrates could be caused by a minority phase as well, which can however not be answered conclusively.

The stability of the self-assembled monolayer of ODPA with respect to competition with water on the studied substrate surfaces was investigated by measuring the contact angle as a function of the immersion time in ultrapure water. After each immersion step of 10 min duration, the samples were dried in a stream of nitrogen and the static water contact angle was measured, characterizing the state of the self-assembly film. The resulting contact angle transients are shown in Figure 3.

Obviously, the static water contact angle on the ODPA covered $Al_2O_3(0001)$ surface was observed to quickly decrease with the time of immersion, finally resulting in a contact angle of 45° which was about that for a bare $Al_2O_3(0001)$ surface. In contrast, static water contact angle measurements obtained for ODPA covered surfaces of both amorphous oxide films and the $Al_2O_3(1\bar{1}02)$ orientation showed constant values of 110°−120° over the tested time of immersion, indicating a stable functionalization with a hydrophobic ODPA self-assembled monolayer. These measurements indicated that the hydrophobic ODPA monolayer after adsorption from ethanol solution forms a dense and self-assembled monolayer as indicated by the water contact angles of 110° and higher. On the polar $Al_2O_3(0001)$ surface, the decrease of the contact angle indicates the dissolution of the ODPA monolayer into the aqueous phase or at least the severe deterioration of the ordered self-assembly film. For all other analyzed surfaces, it was not even possible to decrease the contact angle by immersion in water and simultaneous exposure to ultrasonic acoustic irradiation.

Characterization of ODPA Monolayer Stability by Means of in Situ AFM. The in situ microscopic studies aimed at a more detailed understanding of how the ODPA films desorbed from the $Al_2O_3(0001)$ surface. In situ AFM studies of the ODPA monolayer stability in ultrapure water simulated the situation of the immersion cycles (see above) and allowed for a nanoscopic investigation of the desorption mechanism and stability of the ODPA monolayer on the respective substrates. Even though the substrate is not removed from the solution at any time, the situation is comparable to the contact angle measurements, which are also characterizing the solid/liquid interface. The imaging was done at room temperature and was always done according to the following protocol: First, the surfaces were imaged in a solution of absolute ethanol, which does not lead to desorption of the self-assembled monolayer (the monolayer was formed in this solvent).[39] Subsequently,

(37) Brukman, M. J.; Marco, G. O.; Dunbar, T. D.; Boardman, L. D.; Carpick, R. W. *Langmuir* **2006**, *22*(9), 3988–3998.
(38) Liakos, I. L.; McAlpine, E.; Chen, X. Y.; Newman, R.; Alexander, M. R. *Appl. Surf. Sci.* **2008**, *255*(5), 3276–3282.
(39) Bain, C. D.; Troughton, E. B.; Tao, Y. T.; Evall, J.; Whitesides, G. M.; Nuzzo, R. G. *J. Am. Chem. Soc.* **1989**, *111*(1), 321–335.

ultrapure water was introduced into the cell using a syringe pump. This setup allows for imaging at exactly the same position in different environments (the exact details of the setup were described elsewhere[40]). For the study of the desorption mechanism, the water flow was set to a constant value of 500 μL/min (cell volume about 500−700 μL), which simulated the rinsing of the samples in the immersion cycles.

The first remarkable finding was that the self-assembled monolayer on the $Al_2O_3(0001)$ surface was desorbing immediately after changing from ethanol to water. One has to keep in mind that the solubility of ODPA is much higher in ethanol than in water, which shows that the solubility in this case does not cause such a desorption process. However, as shown in the following, the low solubility of ODPA in water influences the desorption pathway. Topographically, the desorption process could obviously be detected by the formation of islands on the whole surface as can be seen in Figure 4B. Most islands have a height of about 2.3−2.5 nm corresponding to the expected height of the self-assembly film. This clearly indicates residuals of the self-assembly film. Interestingly, some of these islands are spherical in shape and have a height of exactly 2 times the length of an ODPA molecule, indicating the formation of micellelike structures at the oxide/water interface, with one ODPA layer binding to the surface with the phosphonic acid functionality and one physisorbed ODPA layer on top with the phosphonic acid pointing into the solution leading to a hydrophobic alkyl chain core, as depicted in the model in Figure 4. Moreover, the height histogram in Figure 4 shows that these micellelike islands are typically about 50−60 nm wide.

This proves that the adsorption of the ODPA in competition with water is clearly unfavorable on this polar surface, supporting the contact angle measurements. Moreover, the formation of the micellelike islands, which stay adsorbed at the interface, clearly reflects that ODPA cannot dissolve easily into water due to the nonpolar character of the alkyl chain. Hydrophobic interactions between alkyl chains are consequently more favorable compared to adsorption of the phosphonic acid functionality onto the surface. In competition with water, the ODPA molecules can dissolve into the aqueous phase; however, due to the low solubility, they immediately form a second layer on the preexisting ODPA-SAM and stay physisorbed. In order to further support this assumption, the dielectric constant of the medium was lowered again by returning to an ethanol solution. It was observed that the micellelike islands disappeared after changing to ethanol solution as can be seen in Figure 4B. This clearly reflects the fact that the formed ODPA micelles can be dissolved easily into ethanol solutions under such nonequilibrium conditions of a continuous flow. In contrast to the in situ observations on $Al_2O_3(0001)$ surfaces, all other aluminum oxide surfaces did not show any formation of micellelike islands at the interface to the aqueous phase. No desorption of the ODPA molecules could be observed for any of the other aluminum oxide surfaces with the AFM as can be seen in Figures 5 and 6 for the other sample types proving the contact angle studies.

Interestingly, ex situ force-modulated AFM-images of native oxide surfaces on aluminum (type I) before and after immersion in water for 10 min showed differences in the topography as well as phase shifts. In Figure 6C and D, a comparison of AFM topographies for native aluminum oxide surface covered with ODPA before and after immersion into water is shown. The AFM results clearly show a difference in surface topography.

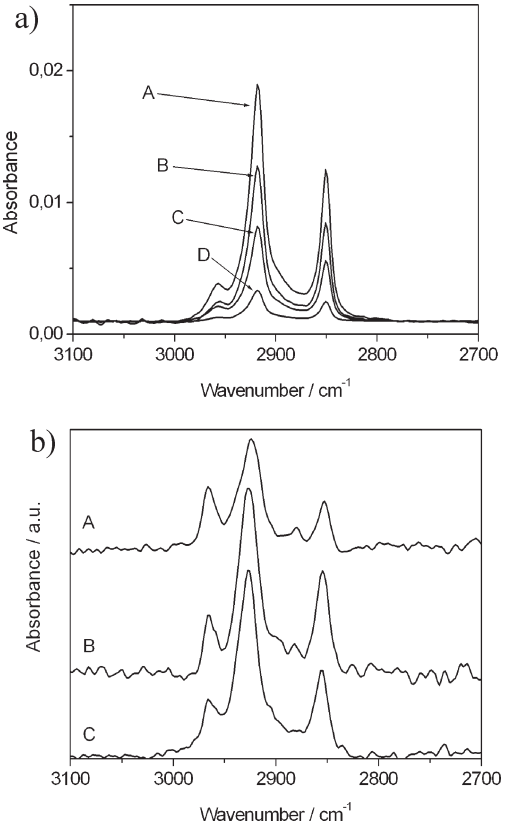

Figure 7. (a) DRIFT spectra of ODPA adsorbed on single-crystalline $Al_2O_3(0001)$ before (A) and after one (B), two (C), and three (D) water immersion cycles. (b) PM-IRRAS spectra of ODPA adsorbed on native grown Al_2O_3 on aluminum before (A) and after (B) one and (C) three water immersion cycles.

We interpret this topographic change as a result of the diffusion of water and oxygen through the monolayer toward the interface, inducing an increase and roughening of the passive film thickness. Since the contact angle did not change and thereby indicated that ODPA is not desorbed from the surface, the growth of the oxide film below the ODPA monolayer seems to occur at the Al_2O_3/Al interface.[15]

In summary, the reported AFM results support the conclusions of the static contact angle measurements, showing that ODPA desorbs only from the polar $Al_2O_3(0001)$ surface. On the other studied surfaces, the ODPA is immobilized on the surface even in competition with water.

FTIR Spectroscopy of ODPA Covered Surfaces after Immersion in Water. The progressive loss of surface coverage could be further confirmed by monitoring the intensity reduction of the characteristic peak heights of the FTIR spectra. As shown in Figure 7a, DRIFT spectra were measured for the ODPA monolayer formed on the $Al_2O_3(0001)$ surface before and after several immersion cycles in water. After the immersion of the SAM in water, the intensity of the peaks corresponding to methylene stretching vibrations was reduced to approximately 20% of the initial intensity. This observation is consistent with the AFM and contact angle measurements, which show monolayer desorption over time with some ODPA remaining on the surface in islandlike structures (see Figure 3 and 4).

In contrast, FTIR spectra which have been obtained for SAMs of ODPA on the other substrates before and after immersion did not show any significant decrease in the peak intensity. Exemplarily, in Figure 7b, the PM-IRRAS spectra are shown for the ODPA film on native amorphous Al_2O_3 covered aluminum. After

(40) Valtiner, M.; Borodin, S.; Grundmeier, G. *Langmuir* **2008**, *24*(10), 5350–5358.

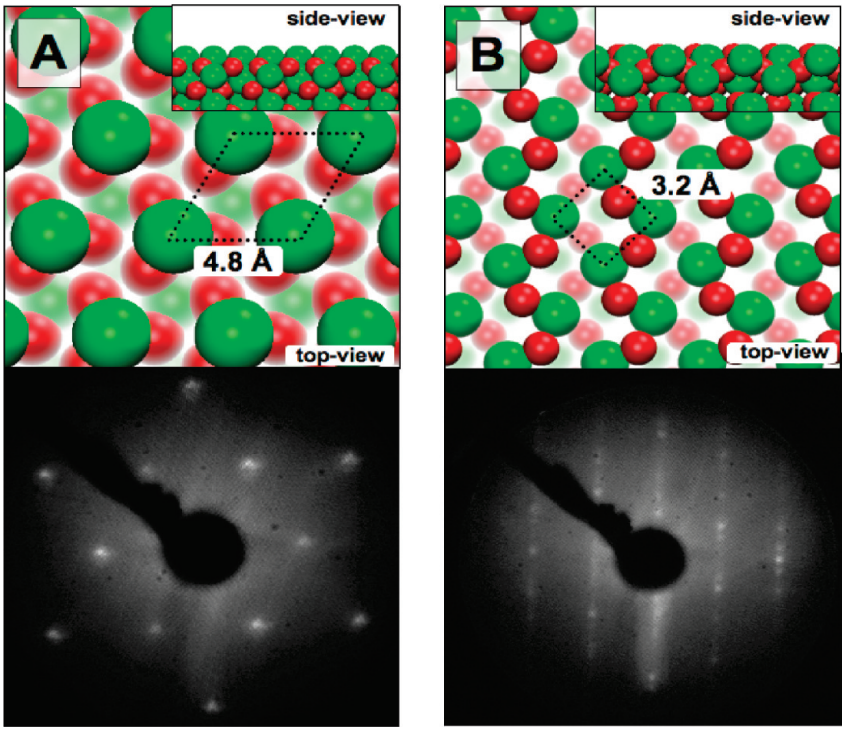

Figure 8. (A) (top) Top view of the atomic structure of the $Al_2O_3(0001)-Al$ surface. The small inlet represents a side view. The polar surface only consists of Al atoms and thus highly reactive Lewis acid sites. (bottom) LEED pattern recorded at 60 eV showing the hexagonal symmetry of the single-crystalline surface. (B) (top) Top view on the atomic structure of the nonpolar $(1\bar{1}02)$ surface. The small inlet represents a side view, showing the nonpolar mixed Al−O termination in the expected ratio. On both surfaces, the spatial arrangements in terms of Al−Al (as indicated) as well as Al−O distances significantly differ. Thus, simple steric arguments discriminate a stable binding of phosphonic acid on the polar surface as well. (bottom) LEED pattern recorded at 87.2 eV showing the cubic symmetry of the single-crystalline surface. It can be seen clearly that the surface additionally exhibits a superstructure into one main direction. The additional spots along the direction suggest either a 4×1 or a 6×1 reconstruction as it was observed in previous studies as well.[48] An alternate explanation leading to this superstructure pattern might be a nonisotropic Ostwald ripening as the surface is annealed (see ref 49). Due to charging problems, it was however not possible to conclusively determine the superstructure. HAS experiments might be a good alternative.[48]

the immersion of the SAM in DI water, the peak height of the CH_2 stretching vibrations were increased while the CH_3 peak areas kept almost constant. According to eq 1, the increase in the CH_2 to CH_3 peak ratio indicates that the mean tilting angle of the self-assembly film increases from 30° ± 0.9° before immersion toward 34° ± 1.2° after immersion, which is also consistent with our AFM results. The AFM results revealed a roughening of the surface due to a corrosive attack at the Al/Al_2O_3 interface explaining the changed peak ratio as observed in these PM-IRRAS studies. After the first immersion cycle, the peak ratio remained constant as well. For the other two surfaces (type II and III), the integral peak intensities remained constant as function of the immersion cycles and no change in inclination angle was found after the immersion cycles.

Discussion

The intriguing question is why ODPA cannot be adsorbed stable onto polar $Al_2O_3(0001)$ surfaces in competition with water but on all other investigated surfaces the binding is stable toward water immersion or at least the surface retains the high hydrophobicity which indicates the immobilization of ODPA at the surface. We think that the three main arguments can explain these distinct behaviors: adsorption free energies of ODPA in competition with water, adsorption geometries, and resulting interfacial types of binding.

First, ab initio thermodynamics[41] and molecular dynamics[24] both predicted that a fully hydroxylated $Al_2O_3(0001)$ surface can be expected as a thermodynamic stable phase at high water chemical potentials, which is in good agreement with experimental studies[29] and our XPS data indicating the presence of hydroxides in the O1s spectra (see Figure 1c). Calculated as well as experimental adsorption energies of water on the Al-terminated $Al_2O_3(0001)$ surface consistently revealed quite high values in the range of 1.1 eV per water molecule. In comparison, on metal surfaces, typically adsorption energies of water are ranging in between 0.1 and 0.4 eV/H_2O.[42,43] On other oxide and hydroxylated oxide surfaces such as, for example, TiO_2, α-quartz, cristobalite, or kaolinite surfaces, values of 0.4,[44] 0.5,[45] 0.5−0.7,[46] and 0.57 eV/H_2O[47] have been reported, respectively. The very high values for the $Al_2O_3(0001)$ surface clearly indicate the highly favorable adsorption of water on the aluminum terminated $Al_2O_3(0001)$ surfaces leading to fully hydroxylated surfaces. Therefore, the adsorption of water on these Al_2O_3-(0001) surfaces is energetically strongly favorable and the resulting hydroxylated surfaces can be considered to be thermodynamically extremely stable.[23] Unfortunately, no values for the adsorption (free) energies of phosphonic acids on the aluminum terminated and hydroxide-stabilized surfaces are available.

(41) Edgar, J.; Chaka, A. M.; Wang, X. G.; Scheffler, M.; Barr, D. *Abstr. Pap. Am. Chem. Soc.* **2000**, *220*, U187–U187.

(42) Ranea, V. A.; Michaelides, A.; Ramirez, R.; Verges, J. A.; de Andres, P. L.; King, D. A. *Phys. Rev. B* **2004**, *69*(20), 205411.

(43) Meng, S.; Wang, E. G.; Gao, S. W. *Phys. Rev. B* **2004**, *69*(19), 195404.

(44) Wendt, S.; Schaub, R.; Matthiesen, J.; Vestergaard, E. K.; Wahlstrom, E.; Rasmussen, M. D.; Thostrup, P.; Molina, L. M.; Laegsgaard, E.; Stensgaard, I.; Hammer, B.; Besenbacher, F. *Surf. Sci.* **2005**, *598*(1−3), 226–245.

(45) Yang, J. J.; Wang, E. G. *Phys. Rev. B* **2006**, *73*(3), 035406.

(46) Tosoni, S.; Doll, K.; Ugliengo, P. *Chem. Mater.* **2006**, *18*(8), 2135–2143.

(47) Hu, X. L.; Michaelides, A. *Surf. Sci.* **2008**, *602*(4), 960–974.

From our experimental results, we however conclude that the adsorption free energy of phosphonic acids onto the aluminum terminated surface as well as onto the hydroxylated polar Al_2O_3-(0001) surface is considerably lower compared to the adsorption energy of water, leading to a desorption of the self-assembly film.

Second, even though there are no thermodynamic data available for the adsorption of ODPA or some other phosphonic acid, an examination of the surface geometry can give a first indication as to why the adsorption energies on the polar surface are much lower in comparison to the other surfaces by simply evaluating the possible steric arrangement of phosphonic acid groups binding on these surfaces. In Figure 8, the atomic structures of the polar and the nonpolar Al_2O_3 surface are depicted. For comparison, the $-PO(OH)_2$ distances within the phosphonic acid group are around 2.8−3 Å. It is obvious that the binding distances of the phosphonic acid are not comparable to the Al−Al distances (4.8 Å) on the hydroxide-stabilized polar surface. In contrast, on the nonpolar $(1\bar{1}02)$ surface, the distances between surface aluminum atoms (3.2 Å) are comparable to the distances in the phosphonic acid. We argue that these interatomic distances are a crucial factor for the formation of a coordinative binding of ODPA toward the alumina surfaces. In particular, oxgygen atoms of the phosphonic acid group, which act as donors for the locally constrained surface aluminum atoms, can donate toward more than one surface aluminum atom only if the nearest neighbor distance is within a reasonable range. The formation of stable bindings between two neighboring surface aluminum atoms and the phosphonic acid group will only be energetically favorable if the interatomic distances match, allowing the coordinative binding of phosphonic acid onto alumina surfaces. By such a condensation reaction, surface hydroxides will be replaced and a stable coordinative binding could be established. The distribution of the hydroxides is not a critical factor for the formation of a strong coordinative binding, as they do not take part in such a binding. Nonetheless, hydroxides seem to have a strong influence on adsorption kinetics on alumina.[16] Consequently, also steric arguments discriminate a stable binding based on a condensation reaction of phosphonic acid onto the polar $Al_2O_3(0001)$ surface. For both amorphous surfaces, it can arguably be expected that a variety of different types of adsorption sites with unsaturated and dangling bonds are present on the surface, allowing for a stable coordinative binding in terms of steric arguments.

Finally, the IR data together with the observed behavior in aqueous solution indicate a weaker bonding of the ODPA toward the $Al_2O_3(0001)$ surface, which is based on purely ionic forces between the phosphonate group and a positively charged hydroxylated surface. It can be assumed that the PO_3^{2-} adsorbs on the protonated hydroxylated $Al_2O_3(0001)$ surface. In contrast, on the other surfaces, additionally P═O stretching modes in the absence of P−OH vibrations could be detected. It can arguably be expected that such an ionic bonding is less stable toward water compared to, for example, an interfacial bonding based on a condensation reaction leading to a direct coordination between the phosphonate group and Al ions. That means for an Al_2O_3-$(1\bar{1}02)$ and amorphous surface that during the adsorption of the phosphonic acid group the surface hydroxyls are protonated and desorb as water from the surface while the phosphonate group is coordinated to the surface Al^{3+} ions. A bidentate condensation would be consistent with the IR data. In Figure 9, a schematic representation of the different binding situations (ionic binding and coordination binding) as present on the various alumina surfaces is shown.

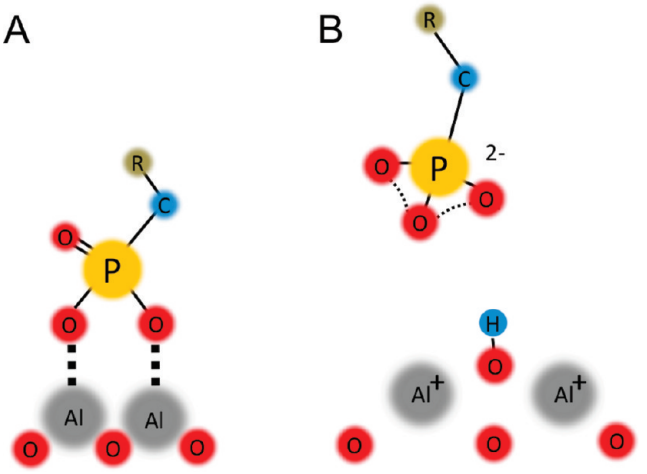

Figure 9. (A) Interfacial binding of a phosphonate group on $Al_2O_3(1\bar{1}02)$ based on condensation reaction and subsequent coordination (if sterically allowed). In the presented case, it is a bidentate binding. (B) Interfacial binding of a phosphonate group on $Al_2O_3(0001)$ based on the ionic attraction between the phosphonate group and the positively charged hydroxylated surface.

Conclusions

In summary, it was shown that the adsorption of octadecylphosphonic acid on aluminum surfaces is based on different types of interfacial bondings between the surface and the ODPA, which strongly depends on the present surface orientation and thereby local geometries. The stability of the resulting bonding is based on three competing influences, namely, interfacial bonding types, adsorption free energies in competition with water, and involved adsorption geometries.

The stability of ODPA self-assembly films toward water was investigated on four different model substrates. This comparative study revealed that ODPA SAMs are stable on (1) native aluminum oxide on a metal support as well as (2) on amorphous aluminum oxide and (3) on $Al_2O_3(1\bar{1}02)$. In contrast, ODPA films are not stable in water on (4) the single-crystalline $Al_2O_3(0001)$ surfaces and immediately form micellelike islands at the solid/liquid interface after immersion. This indicates that the adhesion free energies as well as the local atomic arrangements at the surface play a crucial role for the formation of a stable self-assembly film on aluminum oxide.

In conclusion, the results suggest an extremely important role of the local atomic structure of the aluminum oxide surface with regard to the formation of stable organophosphonic acid films in competition with water. For technological applications, it has to be considered that polar aluminum oxide surfaces should possibly be avoided if high stability of the binding is desired and vice versa. A comparative approach as presented in this work is expected to be valuable not only for the system at hand but also for other relevant systems. The understanding and discussion of the underlying physical driving forces for adhesion and de-adhesion become straightforward based on this differential approach. Moreover, a direct comparison with state-of-the-art ab initio based results is possible.

Acknowledgment. The financial support for P.T. by Bundesministerium für Bildung und Forschung (BMBF) is gratefully acknowledged. The financial support for M.V. by voestalpine Stahl Linz GmbH, Henkel Surface Technologies and the Christian-Doppler Society in Vienna is gratefully acknowledged.

(48) Becker, T.; Birkner, A.; Witte, G.; Woll, C. *Phys. Rev. B* **2002**, *65*(11), 8.
(49) Nguyen, T. T. T.; Bonamy, D.; Van, L. P.; Barbier, L.; Cousty, J. *Surf. Sci.* **2008**, *602*(21), 3232–3238.